Solar Energy Materials & Solar Cells 286 (2025) 113561

Contents lists available at ScienceDirect

Solar Energy Materials and Solar Cells

journal homepage: www.elsevier.com/locate/solmat

Beyond material recovery: Exergy and environmental analysis of silicon solar panel recycling

Šimon Jech [a], Neill Bartie [b], Gulsah Tas [c], Kati Miettunen [d], Rodrigo Serna-Guerrero [c], Annukka Santasalo-Aarnio [a,*]

[a] Department of Mechanical Engineering, School of Engineering, Aalto University, P.O. Box 16100, 00076, Aalto, Finland
[b] Helmholtz-Zentrum Berlin für Materialien und Energie, Hahn-Meitner-Platz 1, 14109, Berlin, Germany
[c] Department of Chemical and Metallurgical Engineering, School of Chemical Engineering, Aalto University, P.O. Box 16100, 00076, Aalto, Finland
[d] Department of Mechanical and Materials Engineering, University of Turku, Vesilinnantie 5, 20500, Turku, Finland

ARTICLE INFO

Keywords:
Solar panel
Recycling
Exergy
LCA

ABSTRACT

The recycling of silicon solar panels is vital to ensure critical material recovery and to sustain the manufacturing of new panels in line with the United Nations Sustainable Development Goals. While various recycling methods based on thermal, chemical, or mechanical separation of the solar panel layers have been studied, a comprehensive thermodynamic and environmental analysis is required to allow holistic comparison within the circular economy framework. Here, such an analysis is performed for four different silicon solar panel recycling processes. First, the processes were simulated in HSC chemistry^{TM} to analyse the flows of exergy. Subsequently, a Life Cycle Assessment (LCA) was conducted to understand the environmental benefits and drawbacks of each method. Combined Exergy-LCA analysis showed that a slightly less exergy-efficient process, namely pyrolysis can ultimately has the lowest environmental impact out of the four processes. In contrast chemical treatment of the encapsulant exhibited comparably worse performance due to its increased resource consumption. On the material level, high-value material recovery, if realized, could be thermodynamically and environmentally advantageous. The recovery methods presented here could be further improved if heat integration or the use of natural solvents would be considered. These unique findings demonstrate that weighing exergy - Life Cycle Analysis trade-offs across different recycling approaches could navigate future developments towards more sustainable solar panel recycling. Therefore, such an approach is recommended over solely focusing on material recovery.

1. Introduction

Solar panels are becoming an essential part of modern energy systems, and they are expanding rapidly. Their growth can partially be attributed to climate mitigation commitments and solar panels have been shown to be the renewable energy source least affected by climate change [1]. Simultaneously, their end-of-life (EoL) treatments are becoming more important [2] as they might cause adverse environmental effects. Sustainable management of materials is advocated for based on SDGs and e.g. recent EU commitments [3]. Circular economy frameworks for solar panel materials are discussed broadly [4–7]. For crystalline silicon solar panels the EoL is particularly important because the panels contain valuable and scarce materials such as silver and solar-grade silicon [8,9] or high-demand aluminium [10]. Broadly speaking, EoL treatment spans from reuse to landfilling [8]. Recycling, the process that recovers useful materials and returns them back into the Technosphere, is the prevailing approach in the EoL treatment spectrum.

Current experimental research on crystalline silicon solar panel recycling focuses mainly on the material recovery aspect. Material recovery starts with the removal of the frame, followed by separation of the parts (glass, cells, polymers) or directly with separation for frameless panels. Separation techniques can be further classified according to the treatment mechanism as thermal, chemical, or mechanical treatment [11].

Thermal treatments utilize elevated temperatures to decompose the

* Corresponding author.
E-mail addresses: simon.jech@aalto.fi (Š. Jech), neill.bartie@helmholtz-berlin.de (N. Bartie), gulsah.tas@aalto.fi (G. Tas), kati.miettunen@utu.fi (K. Miettunen), rodrigo.serna@aalto.fi (R. Serna-Guerrero), annukka.santasalo@aalto.fi (A. Santasalo-Aarnio).

https://doi.org/10.1016/j.solmat.2025.113561
Received 22 October 2024; Received in revised form 24 January 2025; Accepted 3 March 2025
Available online 10 March 2025

encapsulant to separate glass and cells. First of these methods is pyrolysis – decomposition of the encapsulant in a controlled, oxygen free atmosphere at 500 °C [12]. Previously the mechanism and products of Ethylene Vinyl Acetate (EVA), the common encapsulant, pyrolysis were described [12,13]. Huang et al. [14] studied EVA pyrolysis followed by hydrometallurgical treatment and they were able to recover 90 wt% of pure metals and silicon together with around 99 wt% of glass. Similar recovery is achievable via incineration of EVA followed by hydrometallurgical treatment [15]. Both pyrolysis and incineration had the potential to recover intact glass sheets, yet the cells were often cracked [14,15]. These previous findings have indicated a good promise of the thermal separation followed by hydrometallurgical treatment to recover glass and high purity metals and silicon.

Chemical separation of the glass, cell and back-sheet utilizes solvents to break down the encapsulant. The most promising solvent for EVA is toluene [16–18]. Significant challenges exist with this method, as crosslinked EVA swells instead of actually dissolving [19]. Ultrasonication has been proposed to speed up toluene penetration and EVA breakdown [16,18]. This however places further demands on the technical setup and on the supply of chemicals and electricity. While these methods allow recovery of intact cells and glass, they require further treatment to fully separate the encapsulant.

Mechanical separation of the panel parts builds on the traditional recycling based on comminution, phase liberation and subsequent sorting. For example, crushing combined with electrostatic separation of the metals, glass and plastics showed promising results [20,21]. However, it leads to destruction of glass as well as mixing glass with metals and polymers. Furthermore, crushing results in direct material losses through fine dust. On the other hand, it is an established low-cost method and might be more suitable for panels with already broken front glass [20]. Another mechanical process utilized electrohydraulic crushing, which uses high energy pulses in liquids to break down the panels [22]. Crushed panels were then separated in different particle size fractions to concentrate materials. Concentration can be done using screening [22], density separation [17] or electrostatic separation [20]. Lastly, a promising technology for mass separation of glass is so called hot-knife separation which allows the recovery of intact glass sheet via cutting through the top encapsulant layer [23].

Research that compares these methods has chiefly focused on recovery rates [17,24]. Azeumo et al. [17] studied the ultrasound assisted swelling of EVA in toluene (UST) as one method and mechanical crushing combined with density separation as the other. Moreover, authors of the present study previously researched incineration, pyrolysis, and UST experimentally without any conclusive difference in material recovery [24].

Nevertheless, material recovery itself has further impacts, such as its energy consumption and environmental footprint. Minimization of these impacts is essential in striving for sustainable and circular solutions [25–27]. There is no argument against the fact that recycling should recover as much materials as possible and this is reflected in policies [9]. However, from a thermodynamic perspective, the more is recovered the more resources and energy need to be invested [28]. To navigate this dilemma in recycling, exergy analysis [29,30] becomes a valuable tool. Exergy analysis allows description of energy inputs based on their thermodynamic quality; chemical exergy allows allocation of exergy to materials in similar fashion [31].

Exergy analysis has already proven to be valuable in optimizing car recycling [30]. More recently similar approach was used to highlight exergy losses across the whole solar panel value chain [32,33]. They also incorporated life cycle assessment (LCA) in a later publication [34] and demonstrated that closed loop recycling can be environmentally beneficial.

Environmental impacts of recycling are important to assess as secondary materials should not bear higher impacts than primary ones. Thus, LCA of recycling is as important as exergy analysis [6,35]. LCA of pyrolysis-based silicon solar panel recycling was conducted, listing impacts from transportation of EOL panels to metal recovery [36,37] as well as to simulate process scale-up [38]. Recently an overview of LCA on silicon solar panel recycling was published, which argued - among other things - that the main LCA focus of published studies was on the levels of recycling (e.g. reuse of panels, revival of panel parts or material recycling) [39]. Heiho et al. [40] presented a comparative LCA for different mechanical recycling techniques of solar panels in Japan. A similar approach was taken by Dias et al. [41], focusing on solvent treatment. Both proved that it is possible to conduct early-stage LCA on pilot-scale or laboratory-scale methods.

Still, there is a gap in understanding both the thermodynamical and environmental impacts of thermal, chemical, or mechanical separation methods. Previous research is limited to evaluating either the thermodynamical or environmental impacts or to one set of recycling or separation methods.

Considering the findings presented in this work, its novelty lies in the comparison of solar panel separation techniques to demonstrate the importance of evaluating the exergy and environmental impacts simultaneously while seeking sustainable solutions. Different silicon solar panel recycling processes are explored - namely incineration, pyrolysis, ultrasound assisted swelling of the encapsulant in toluene and mechanical recycling - from the material recovery, exergetic and environmental perspective, which has not been done before in one study. This comparison is done by simulating the four processes in HSC chemistry™ [42] software, and subsequently using OpenLCA [43] with Ecoinvent 3.8 [44] to conduct LCA based on the inventory data gathered in the simulation. The presented theoretical comparison of recycling pathways provides foundations for future decision making, industrial actions and studies of social impacts.

In the following section the methodology is outlined. Then, the results of the detailed exergy analysis for the 4 different processes (one of which has 2 variants, resulting in total of five analyses) are described. Next, the LCA is presented and discussed. Finally, general discussion connects the observations from the exergy analysis and the LCA and shows the importance of using both techniques in assessing the recycling processes.

2. Materials and methods

2.1. Process definition

Recycling processes of silicon solar panels were at the core of this work. Four different separation processes (five in total, when the two variants of ultrasound assisted swelling of the encapsulant in toluene (UST) are considered) were analysed and compared based on environmental and exergy footprints.

1. Incineration
2. Pyrolysis
3. UST
   a UST-vol. – volume-based toluene consumption (see details in section 2.6.4)
   b UST-exp – experimental-based toluene consumption
4. Mechanical recycling combined with incineration.

Fig. 1 details the analysed processes together with their respective boundaries. The boundaries and streams are coloured distinctly for each process with some stages shared between all or some of the processes (e.g. dismantling and glass separation, respectively). Streams crossing the boundaries are either end products or emissions to the environment, except the cell residues which are further processed.

2.2. Quality and recovery assumptions for target materials

The recovered useful products were Ag, Cu, SnO_2, PbO_2, aluminium alloy, solar grade silicon and glass in all the processes. Pure silver and

copper could be sold for smelting and direct reuse. Acceptance of recycled solar-grade silicon is yet to be fully studied. However, in principle it's reuse is possible [14,45,46]. Glass was assumed as recovered in useful form (un-broken solar-glass sheet) in all processes except the Mechanical process. Thus, material recovery for each process could be calculated as follows:

$$\text{Material recovery} = \frac{\sum m_{i;out}}{\sum m_{i,in}} \quad (1)$$

Where $m_{i;in}$ and $m_{i;out}$ are the masses of the material in the feed and the masses of recovered useful products respectively. Detailed feed composition, composition of recovered useful products, and the composition of each stream are presented in Supplementary Tables S8 and S9 and Supplementary file 2. For simulation purposes the purity of recovered silver and copper was assumed to be 100 %, while tin and lead were recovered in 100 % pure oxide-form. The recovered silicon was also assumed to be 100 % pure by omitting the residual trace elements in the recovered solar grade silicon, following the findings of Huang et al. [14]. Conditions and assumptions for silicon and metal recovery simulations were kept identical for each of the five simulated process variants, as detailed in section 2.7.5.

2.3. Exergy analysis

Accounting for material degradation and energy expenditure is vital to understanding the differences between recycling processes. Real processes usually dissipate some amount of energy and thus the entropy of real systems increases. Furthermore, entropy increases when materials get mixed or contaminated.

Therefore, employing a tool which enables the description of material transformations together with material and energy losses becomes useful. Exergy analysis is such a tool. Exergy refers to the useful work which can be extracted from flows of energy or matter; thus, it is also known as available energy. Through exergy analysis energy dissipation during the recycling process can be accounted for [31]. Furthermore, exergy analysis describes material transformations during recycling and helps quantify the loss of materials via waste streams [30].

Exergy analysis performed in this work was based on the concept of chemical exergy introduced by Szargut et al. [31], which had been implemented in the HSC chemistry™ software:

$$Ex_{tot} = \sum_i n_i b_i^{ref} + \Delta G_f^0 \quad (2)$$

where n_i is the number of moles of an element in the species, b_i^{ref} is the exergy of the reference element, and ΔG_f^0 is the standard Gibbs free energy of formation. This was used to calculate the exergy of all materials and chemical streams entering and leaving the system. As the simulation considered continuous streams (expressed as mass per unit time), the exergy was expressed as exergy rate (kJ/s, i.e. kW). Finally, the exergy of heat was based on Carnot's efficiency:

$$Ex_{heat} = Q\frac{T}{T_0} \quad (3)$$

Where Q is the amount of heat T is the temperature of the stream and T_0 is the standard temperature of 298.15 K. The software also accounts for other forms of physical exergy via enthalpy and entropy changes [47]. Furthermore, exergy of electricity was assumed equal to the electrical energy supplied and it was assumed to be dissipated as heat to balance the enthalpy over the unit operations. Details of assumed energy supply and dissipation are described in section 2.7.

Heat loss further contributed to irreversibility since heat is assumed to be fully dissipated at the standard temperature of 298.15 K, resulting in no exergy content by convention. Exergy loss due to mixing was omitted in this analysis since it was not implemented in the software used and most of the processes do not primarily mix materials. Thus, only the exergies of streams are used for this study, similarly to Refs. [48,49].

Finally, the irreversibility over each unit operation was calculated based on:

$$I = \sum Ex_{input} - \sum Ex_{output} \quad (4)$$

Where I is the irreversibility and Exinput and Exoutput are the values of exergy (chemical, physical, heat, and electricity) entering and leaving the unit operation respectively.

2.4. Exergy efficiency

Additionally, the overall exergy efficiency of each process was calculated as the ratio of the exergy of the recovered target useful materials and the exergy of all the inputs (end-of-life panels, chemicals, electricity, heat) [30]. The ratio can be written as:

$$\eta_{Ex} = \frac{\sum Ex_{recovered}}{\sum Ex_{input}} \quad (5)$$

2.5. Exergy of EVA

Thermodynamic properties of most materials used in monocrystalline silicon solar panels were well described in the simulation software and the exergy content was determined from equation (1). The major exception was the EVA polymer, for which data were scarce as it is a complex hydrocarbon. Therefore, the exergy content was determined based on semiempirical correlations presented by Van Krevelen et al. [50], similarly to Ignatenko et al. [30]. The detailed approach is compiled in Supplementary material S1. Based on the chemical structure of EVA the Gibbs free energy of formation was determined as $\Delta G_f^0 = -9058 \frac{kJ}{mol}$. This approximation mirrors a single chain long molecule without crosslinking. Ultimately, this resulted in an Exergy content of 41.96 MJ/kg. Furthermore, empirical correlations were utilized to validate the assumed exergy content. Based on correlations of Kotas [51] the EVA exergy content would be 39.36 MJ/kg or 39.39 MJ/kg based on Tang et al. [52], for details see Supplementary material S1. This validated the semiempirical approach presented and thus it was implemented in the simulation software.

2.6. Life cycle assessment

The LCAs for the different recycling routes were performed by using OpenLCA 2.0.3 [43] software and the Ecoinvent 3.8 database [44]. The goal and scope of these analyses was to compare the environmental benefits and drawbacks of the five variants of the four processes (UST-vol and -exp., Incineration, Pyrolysis and Mechanical process) to identify the least harmful recycling approaches. Furthermore, the functional unit was determined as: "recycling of 1 ton of silicon solar panels in Europe" with the defined processes.

The life cycle inventory was compiled on the process level by drawing the system boundaries in a grave-to-gate approach starting from the dismantling of solar panels until the end of the neutralisation step for all processes, as visualized in Fig. 1.

Since solar panels include many different valuable materials that can be considered as a product at the end of the recycling process, a multifunctionality problem had occurred for the evaluation of environmental impacts. This problem was solved by the substitution approach where the recovered target useful materials (glass, aluminium alloy from the frame, Ag, Cu, SnO_2, PbO_2 and Solar-grade silicon) were considered as the replacement of their possible primary production. Consequently, the recycling of solar panels contributed to avoiding the environmental impacts of their primary production. Therefore, the recycling benefits can be observed as negative values which indicate the avoided environmental impacts.

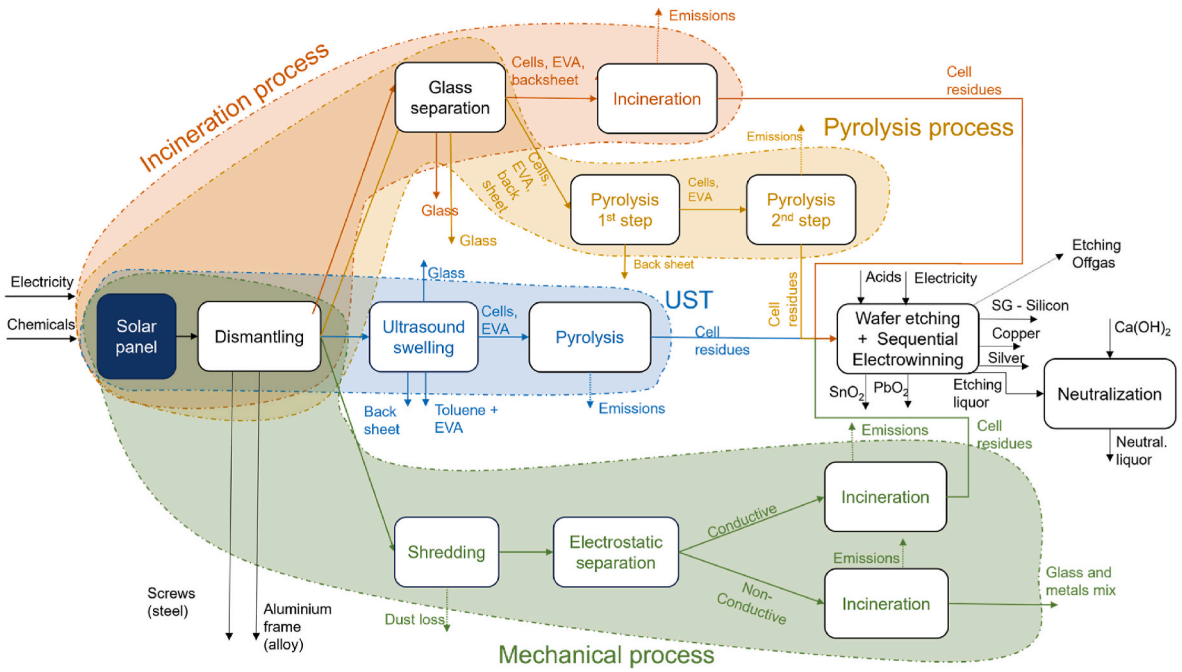

Fig. 1. Process boundaries and unit operations of the simulated recycling processes, (SG-silicon – solar grade silicon). (For interpretation of the references to colour in this figure legend, the reader is referred to the Web version of this article.)

However, for some of the byproducts (such as copper and tin oxide recovered by wafer etching), the direct replacements of the recovered products were not found in the database. Therefore, their mineral concentrate was chosen as a substitute on a recovered metals-basis. The details of the product streams selected for the processes together with the life cycle inventories are given in Tables S3–S7 in the supplementary material. Upon completing life cycle inventory, impact calculation was carried out by using the ReCiPe 2016 Midpoint (H) methodology in 16 different categories.

2.7. Process simulation and conditions

Four different processes were simulated to expand on previously published simulations of incineration-based recycling [32]. This simulation was expanded by introducing pyrolysis, UST or crushing plus electrostatic separation processes respectively. This expansion was based on published data for pyrolysis [12,13] and mechanical process [20]. In contrast, the UST process was based on author's experimental data [24]. Initial input of the EoL panels was set at 1000 kg/h to be able to compare to previously published results [32,36] and the processes were assumed to run in one batch. Detailed process conditions are listed in Supplementary Table S10. The electricity consumption for heating steps (e.g. pyrolysis oven, incineration oven, toluene preheating) was assumed based on enthalpy balance over the respective unit with the assumption of no heat losses to the environment.

2.7.1. Incineration

The process including incineration of the polymers was previously discussed and simulated by Bartie et al. [32], and the process conditions adopted herein can be found in Supplementary Table S10. Additionally, the products of the incineration step were assumed to cool-down to 25 °C to account for heat loss.

2.7.2. Pyrolysis

In this study, the process simulation was based on the process described by Wang et al. [12]. A two-stage process was assumed where the panel sandwich was first heated to 150 °C to soften the EVA and to recover the back-sheet while avoiding fluorine release. Here, it was assumed that 100 wt% of the back-sheet was separated and 100 % of EVA remained with the cells and carried on to the second stage - pyrolysis at 500 °C in a nitrogen atmosphere. De-Wen et al. [13] and later Wang et al. [12] assessed the products of EVA pyrolysis experimentally: both state that the first reaction step was the deacetylation of the EVA. During deacetylation acetic acid is released which can subsequently further decompose into gaseous CH_4, CO_2, CO and H_2 [13]. This decomposition path was implemented in the simulation together with the collapse of the initial long chain into smaller molecules based on the proposed chain scission mechanism [12]. Thus, it was assumed that the final products of the polymer chain decomposition were C_3H_8, C_3H_6, and C_4H_{10} and these formed the pyrolysis liquor, detailed composition of which can be found in supplementary material S11. Such a detailed product description was necessary to accurately estimate the irreversibility of the pyrolysis stage. The minimum required energy was supplied in the form of electricity and was estimated based on the enthalpy balance over the pyrolysis oven. The permanent gas, pyrolysis liquor, and cell residues were cooled down to 25 °C, to allow for the determination of the heat loss during the process.

2.7.3. Mechanical recycling combined with incineration

For the process of mechanical recycling combined with incineration, the simulation included panel shredding and electrostatic separation. Data on copper, silver, silicon, glass as well as polymers recovery and energy consumption were taken from Ref. [20]. The adopted simulation data are detailed in Table S12. Shredded panels were assumed to be separated into conductive and nonconductive fractions through electrostatic separation, as visualized in Fig. 1. Subsequently both fractions were subjected to incineration to decompose the organic materials. The conductive fraction containing most of the metals and silicon further went to wafer-etching to recover metals and silicon (see section 2.7.5.)

2.7.4. Ultrasound assisted swelling of the encapsulant in toluene

The last constructed model simulated the UST process. To construct this model, experimental data on the consumption of toluene and ultrasound power was used [24]. In Fig. 1 Ultrasound swelling (US-swelling) represents the ultrasound bath and its operation. For the UST process, the main input was electricity, the consumption of which was

estimated based on the 300 W per 18 l of liquid applied in Ref. [24]. The second input was based on the experimental consumption of 20 ml of toluene per gram of panel sample (UST-exp) which resulted in a consumption of 16.48 m^3 of toluene per the mass (824 kg) of treated panels. Accordingly, the electricity consumption was 302.2 kWh for 1 h of treatment. As this consumption is excessive a second assumption for toluene consumption was studied. Assuming a mature process would optimize the toluene consumption a second variant was simulated. The second variant assumed immersion of the panel in a volume of toluene three times the volume of the panel itself (UST-vol). This assumption resulted in a consumption of 2.945 m^3 of toluene and 53.99 kWh of electricity per 824 kg of panels treated (for further details, see supplementary material S7). The fraction of EVA which remained on the cells was 50 wt% of the initial EVA mass; the rest of the EVA was dispersed in toluene and was considered as waste. It needs to be stressed that toluene itself is a hazardous compound [53], and related health risks must be controlled.

2.7.5. Silicon and metal recovery

The simulation of silicon and metal recovery included silicon wafer etching to remove metals and the anti-reflection, passivation, and rear-contact layers of the solar cell, followed by sequential electrowinning of metals as proposed by Huang et al. [14]. The process sequentially recovered silver (99 % pure) and then copper (99 % pure) from the acid solution obtained during etching with recovery rates of 77.4 wt% and 83 wt% respectively. Furthermore, tin precipitates as SnO_2 and lead deposits on the counter electrode as PbO_2. Roughly 90 wt % of silicon was also recoverable in the form of solar grade silicon. The residual etching liquor was neutralized using $Ca(OH)_2$ in the neutralisation step [32].

3. Results

3.1. Mass-based material recovery

To illustrate which materials could be recovered, material recovery was calculated for pure metals, silicon, and glass for the different recycling technologies using equation (1) (see section 2.1), bearing in mind the assumed material purities (see section 2.7.5). The results are presented in Fig. 2, it unveils that UST, pyrolysis and incineration could achieve the same recovery in the simulated processes. Imperfect recovery of metals, especially silver (70 wt%) and copper (78 wt%), was due to the inefficiency in the wafer etching process. Secondary losses occurred during the thermal decomposition of the polymers, where part of the cells was assumed to be lost in ashes or dust. Similarly to metals, silicon was mainly lost during wafer etching, where the emitter layer was etched off together with the antireflection and passivation layers. This resulted in a silicon recovery of 87 %, which is still higher than that of metals. In contrast, the material recovery of aluminium was quite high (98 wt%) because most of it is contained in the frame which was recovered as-is in the dismantling step. The remaining aluminium loss stemmed from wafer etching. Finally, glass is assumed to have a theoretical 100 wt% recovery, as it could be recovered as a whole sheet and processed for reuse during glass separation and US-swelling. However, further material losses are to be expected during glass treatment, e.g. through breakage or abrasion. Reuse of glass did not apply to the mechanical process where the glass was recovered in culets mixed with metals and part of it was lost during shredding as well, thus not the same quality as in other processes.

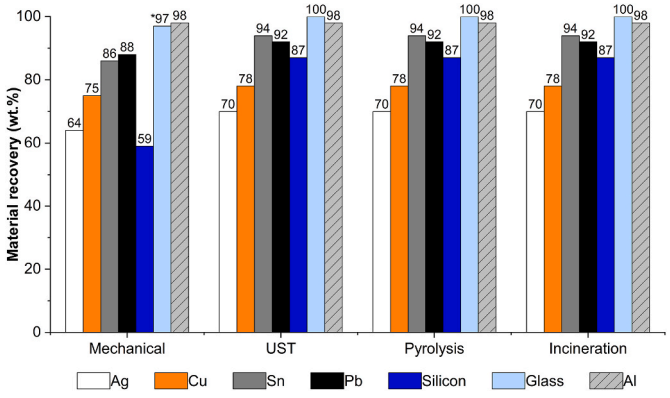

Fig. 2. Mass-based recovery of the target valuable materials. The bars show the assumed percentage of materials recovered through each of the four simulated processes. Values on top of the bars show the actual weight percentage of the initial material input recovered through each process, following equation 1. (*recovered as culets – not the same quality as other processes).

Furthermore, Fig. 2 shows that the mechanical process achieved the lowest recovery among all processes. The lower recovery was mainly caused by the dust loss during shredding (2.95 wt% of the initial mass), which decreased especially the glass recovery compared with the other processes. Further losses could be attributed to inefficient material separation in the electrostatic separator, for instance to metals being discharged in the nonconductive fraction. The most significant decrease in recovery occurred for silicon (59 wt% recovered), which was mainly due to the inefficient electrostatic separation. While the recoveries presented here are based on literature data and partly assumptions, they are reasonably accurate for the following exergy and environmental analysis.

3.2. Exergy flows

The flows of exergy were mapped to establish the exergetic footprint of the processes. Through this exercise, recovered materials with high exergy content could be pinpointed, processes that dissipate exergy irreversibly could be identified, and the proportion of the initial exergy that ended up in waste streams could be calculated. A Sankey diagram in Fig. 3 illustrates the flows of exergy in the pyrolysis process – the corresponding diagrams for the other processes can be found in Supplementary Figs. S1–S4.

As can be seen, the aluminium panel frame had the highest single contribution (~1417 kW) of directly recovered materials. A significant proportion was also recovered in the silicon wafers (235 kW) and the glass (171 kW). Moreover, metals in form of pure silver and copper together with SnO_2 and PbO_2 were recovered as well, but with the lowest contribution to the recovered exergy (5 kW) as the initial content – and thus the recovered mass – was low. A considerable amount of exergy (333 kW) was contained in the back-sheet. However, it is unlikely that this could be reused as-is and further treatment would be necessary. Overall, the main losses stemmed from the products of pyrolysis – the condensed fraction (liquor – 724 kW) and the permanent gases (75 kW). The total irreversibility in the pictured pyrolysis process was 238 kW and the contributions of each stage are discussed in detail in the following section. Apart from the EoL panels (3017 kW) most of the input exergy flowed in with the electricity (140 kW) and heat (40 kW). Finally, the input of chemicals generally had an order of magnitude lower exergy content (2–16 kW) as their required mass was low. In summary, process inputs such as electricity and chemicals lose their exergetic quality during the operations and thus contribute to irreversibility.

Supplementary Figs. S1–S4 put on display the flows of exergy of all the other simulated process variants. A key difference between the processes was the magnitude of secondary inputs: for instance, UST had higher exergy inputs via toluene and electricity, and toluene also constituted a significant waste stream. On the other hand, the mechanical process consumed a similar amount of exergy inputs, but there was a loss of exergy via dust. Finally, incineration had the lowest input exergy flow, as the oxidation of the EVA itself was exothermic [54], so no additional input energy was assumed to run the incineration oven,

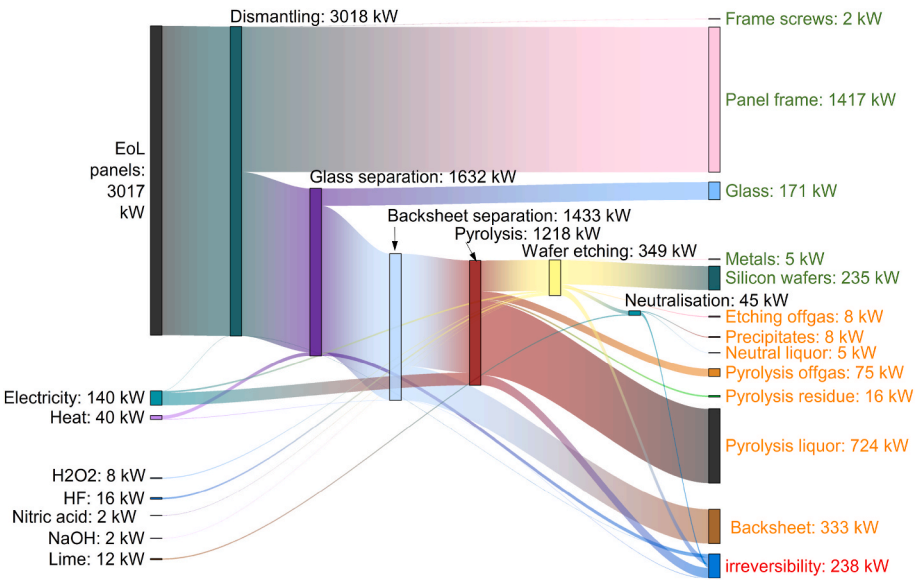

Fig. 3. Sankey diagram of the exergy flows for the simulated pyrolysis process. The left-hand side shows the input exergy of EoL panels along all other inputs, whereas outputs are shown on the right-hand side (useful materials highlighted in green, exergy losses in red and material losses in orange). The figure also shows the flow of exergy through each stage. (For interpretation of the references to colour in this figure legend, the reader is referred to the Web version of this article.)

purely based on the enthalpy balance over the process. Incineration also dissipated less exergy through waste streams, but the irreversibility was greater than that for pyrolysis or UST. However, there are more aspects to exergy losses and irreversibility, and these are now discussed farther.

3.3. *Irreversibility analysis*

Zooming in to the flows of exergy presented in Fig. 3 and Figs. S1–S4, one could have seen that each unit operation contributed to the irreversibility. Fig. 5 visualizes where the irreversibility arose.

Comparing the processes on Fig. 4 makes it evident that the incineration or pyrolysis unit operations contributed the most to irreversibility in almost all variants. The only exception was the UST-exp variant where the US-swelling had a higher contribution. It is also clear that the Mechanical and Incineration processes had a significantly larger proportion of exergy lost during combustion compared with the equivalent pyrolysis steps of the other three variants. The simulations further indicated that the incineration dissipated around 35 % of the initial EoL-panel exergy content while pyrolysis dissipated only around 3 %. This was because the pyrolysis products had higher exergy content, yet to obtain these products electricity input was required which contributed to irreversibility. The larger energy dissipation in incineration could be attributed to the exothermic combustion reaction which was required to sustain the incineration unit operation. On the other hand, the mixture of off-gases and the pyrolysis liquor had no reported use and the most convenient treatment would have been incineration for heat recovery. This would increase the irreversibility and bring it closer to the combustion-based processes, but this was out of this work's scope.

The second major source of irreversibility were steps which included chemical reactions. These were wafer etching and neutralisation, where the products generally had lower exergy content, and the reaction heat was dissipated. Furthermore, the US-swelling step contributed significantly to the irreversibility of the UST processes. Losses during this step arose from the use of electricity and its dissipation during the unit operation. As seen from Fig. 4, the scale of the irreversibility loss in UST was highly dependent on the amount of toluene, which directly influenced the magnitude of electricity consumption.

Similarly, the crushing step contributed notably to the irreversibility during the mechanical process. Once more, irreversibility arose from the use of electricity. In contrast the electrostatic separation allowed

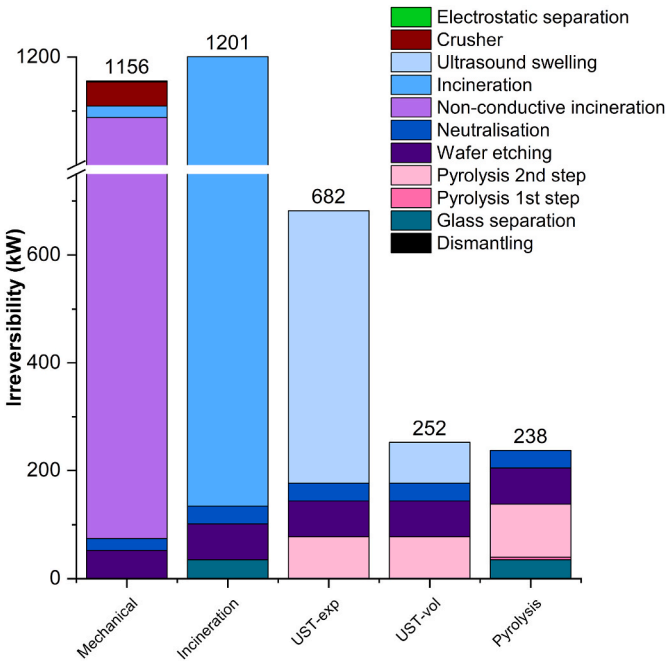

Fig. 4. Simulated irreversibility breakdown for all processes. The stacked bars show the contribution of each stage towards the irreversibility, colour coded according to the legend in the top right corner. On top of each bar is the cumulative irreversibility for each of the process variants. (contributions of some stages might not be visible due to their small magnitude). (For interpretation of the references to colour in this figure legend, the reader is referred to the Web version of this article.)

material separation at low loss of exergy. However, these two are dependent steps and were further analysed in conjunction.

At this stage it is useful to compare the steps preceding the thermal treatment (pyrolysis or incineration) as these constituted the major difference between the five process variants, see Fig. 1. Hence, in a decreasing order of irreversibility, these processes compare as follows: US-swelling (75.55 kW or 505.4 kW, UST-vol or UST-exp, respectively), crushing and electrostatic separation (45 kW and 1.896 kW), and glass

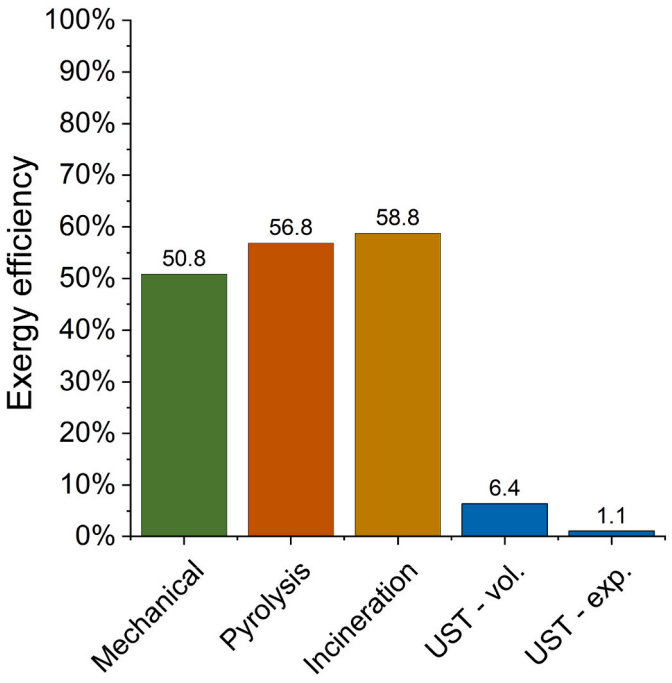

Fig. 5. Comparison of theoretical exergy efficiencies across the simulated processes. Values on top of the bars indicate the exact efficiency value.

separation (34.06 kW). This result highlights that UST would have been the process with the highest exergy destruction and simultaneously having the highest material inputs. However, UST exhibited the benefit of back-sheet recovery. In contrast, the assumed hot knife glass separation exhibited the lowest loss. Crushing and electrostatic separation fell in between these two extremes. Despite this, crushing and separation caused direct material loss, and mixed the glass with other components, which hinders the material recovery as shown in Fig. 2. In summary, while Ultrasound swelling, glass separation and crushing served a similar purpose, the relatively low exergy destruction meant that hot knife separation of glass was the most beneficial approach, whereas the use of UST is hard to justify given the high toluene consumption.

Finally, the dismantling step (i.e., the removal of the frame in the very beginning of the processing) turned out to be an efficient operation from the exergy point of view. During dismantling only relatively low amount of electricity was used and the frame was efficiently separated. In conclusion there are unavoidable irreversible losses in the processes. However, it is instructive to look at how these translate into process efficiency in the following section.

3.4. Exergy efficiency

To provide more clarity, the exergy efficiency of the simulated processes is presented in Fig. 6. Exergy efficiency was defined as the ratio of recovered exergy through recovered useful materials and the initial exergy inputs in EoL panels plus all the needed resources (see Equation (5)).

From Fig. 5 it becomes evident that the UST processes have the lowest exergy efficiency among the simulated processes. Hence, from a thermodynamic perspective only 1.1–6.4 % of the exergy input is recovered and the rest is lost. In turn Pyrolysis and incineration are within 2 %pt. from each other, (56.8 % and 58.8 % respectively) signalling similarly efficient processes. The most profound difference between these thermal processes is the substantially higher electricity consumption in the pyrolysis process, which would explain the lower efficiency. The mechanical process is less efficient (50.8 %) as the glass is not recovered in its pure form but mixed with metals – thus not assumed as useful product.

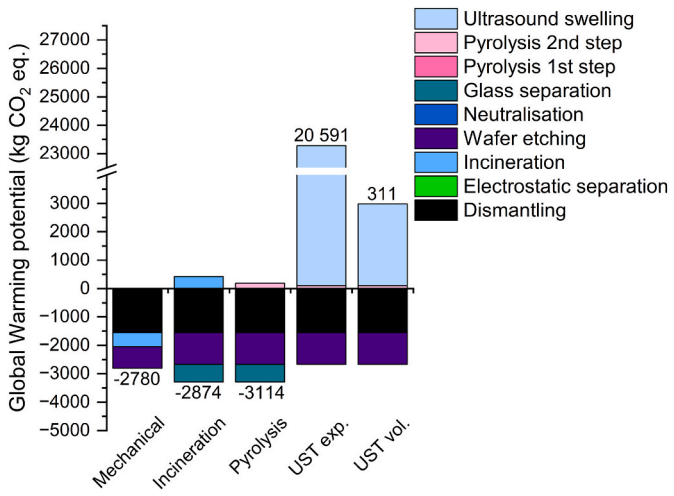

Fig. 6. Global warming impact potential per each unit operation of the 5 simulated variants based on the ReCiPe 2016H Midpoint methodology. Bars bellow the x-axis indicate net-avoided environmental impact per given operation; bars above x-axis indicate net increased impacts. In similar fashion numbers below and above indicate the cumulative avoided environmental impact *(negative number)* or generated *(positive number)* additional impacts *(the numbers do not correspond with the scale as they depict the sum of all the avoided and generated impacts)*.

Focusing on the UST processes, the main reason for such a low efficiency was the high volume of toluene used, which was assumed to be discharged as waste material. This meant that there was a high chemical exergy input compared to materials directly recovered. In contrast, the thermal processes required much less chemicals or process gases and thus turned out to be more exergy efficient. Subsequently, the mechanical process lost the exergy in dust, or the glass mixed with metals, which is analogous to previous findings [30,55,56]. However, for all the processes, the highest loss was attributed to the decomposition of the plastics which initially carried large amounts of exergy. The loss occurred either through dissipation of electricity or via combustion or thermal decomposition during incineration or pyrolysis respectively. Furthermore, the products of pyrolysis or incineration were assumed to leave the process as losses, thus lowering the efficiency significantly.

3.5. Environmental impacts

Analysis of environmental impacts according to the ReCiPe 2016H methodology is presented in Table 1 based on the inventory data reported in Supplementary Tables S3–S8. Negative values in the presented data reveal that all the process variants, resulted in some degree of avoided environmental impacts, indicating that recovery of the useful products (Cu, Ag, SnO_2 and PbO_2, aluminium alloy, solar grade silicon and solar glass), had lower impacts than primary sourcing of such materials. Only the UST-vol. resulted in increased environmental impacts in water consumption, fossil resources scarcity, global warming and freshwater ecotoxicity impact categories respectively, while UST-exp. could generate additional environmental impacts in fine particulate matter formation, both ozone formation categories and terrestrial acidification, possibly due to the high amount of toluene usage and emission. Detailed summary of impacts per stage for the five process variants is included in Supplementary Tables S12–S15.

If the focus is shifted to one of the most examined environmental impact categories –the global warming potential (GWP) – a unit-based comparison in Fig. 6 reveals that incineration and pyrolysis avoids more impacts than the mechanical recycling process. Pyrolysis avoids the most impact (−3114 kg CO_2 eq.), due to reduced gaseous emissions, especially CO_2, from pyrolysis treatment compared to incineration (−2874 kg CO_2 eq.) Even though the incineration process caused direct

Table 1
LCA impact values based on recycling of one ton of solar panels for the five simulated processes, following the ReCiPe 2016 Midpoint methodology.

	Unit	Mecha-nical	Incine-ration	Pyro-lysis	UST exp.	UST vol.
Fine particulate matter formation	kg PM2.5 eq	−6.9	−7.4	−7.6	6.7	−5.5
Fossil resource scarcity	kg oil eq	−781.2	−888.6	−882.7	18591	1978.6
Freshwater ecotoxicity	kg 1,4-DCB	−221.0	−235.4	−249.0	1771.6	47.9
Freshwater eutrophication	kg P eq	−1.6	−1.8	−1.9	−1.8	−1.9
Global warming	kg CO_2 eq	−2780.8	−2874.2	−3114.1	20591	310.5
Human carcinogenic toxicity	kg 1,4-DCB	−436.4	−453.9	−465.2	−191.4	−426.6
Human non-carcinogenic toxicity	kg 1,4-DCB	−9320.2	−10012	−10212	−8441.7	−9987.0
Ionizing radiation	kBq Co-60 eq	−318.4	−411.6	−468.7	−478.0	−482.7
Land use	m2a crop eq	−75.3	−86.9	−90.3	−90.2	−91.0
Marine ecotoxicity	kg 1,4-DCB	−303.0	−322.9	−342.3	−251.2	−330.5
Marine eutrophication	kg N eq	−0.1	−0.2	−0.2	−0.1	−0.2
Mineral resource scarcity	kg Cu eq	−82.0	−91.9	−92.3	−91.0	−92.2
Ozone formation, Human health	kg NO_x eq	−5.4	−9.8	−9.0	25.2	−4.4
Ozone formation, Terrestrial ecosystems	kg NO_x eq	−3.4	−10.2	−8.7	28.2	−4.0
Stratospheric ozone depletion	kg CFC_{11} eq	0.0	0.0	0.0	0.0	0.0
Terrestrial acidification	kg SO_2 eq	−13.9	−15.0	−15.3	28.3	−9.0
Terrestrial ecotoxicity	kg 1,4-DCB	−7521.0	−7819.8	−8332.8	−36.6	−7150.1
Water consumption	m^3	−34.3	−39.3	−40.6	451.9	31.0

release of CO_2 emissions from EVA combustion, the recovery of materials outweighed the environmental impacts created during the process. Although the mechanical process combined with polymer incineration demanded less resource and energy input than pyrolysis, material loss during crushing and separation resulted in less recovered materials and thus less avoided impacts (−2780 kg CO_2 eq.) compared to pyrolysis and incineration.

While these three processes helped avoiding environmental impacts in the GWP category, additional impacts could be generated via both UST processes (20 591 kg CO_2 eq,. for UST-exp. and 310.5 kg CO_2 eq for UST-vol.). This can be directly linked to the US-swelling unit operation with its high toluene and electricity consumption, as seen from the respective bar in Fig. 6. While the possible optimization of the amount of toluene used (UST-vol.) implied significant improvements, it still resulted in increased environmental impacts.

Fig. 6 also shows that the layer separation units themselves (crushing + electrostatic separation, combustion, pyrolysis and US-swelling) resulted in some degree of negative environmental impacts, while the other steps possessed net environmental benefits. Although, in addition to consuming electricity and chemicals, there was no direct recovery from the separation steps, they were vital to liberating the materials contained in the panel. On the other hand, it can be seen from Fig. 6 that the US-swelling unit operation was disadvantageous compared to the others. In contrast, crushing and electrostatic separation seems to have generated less harm, but it also decreased the overall performance of the mechanical process. Interestingly, the incineration unit of the mechanical process avoided some GWP impacts, while all the other incineration or pyrolysis steps generated impacts. This can be explained by glass recovery through the incineration step in the mechanical process, which outweighed the negative impacts of gaseous emissions.

In addition to global warming potential, mineral resource scarcity was also examined in detail, as shown in Fig. 7, considering its importance in assessing mineral resource savings through recycling. From the comparison in Fig. 7, mechanical separation results in least avoided impact (−82 kg Cu eq), because of the reduced avoided impact in wafer etching and increased impact via combustion. This outcome relates to the direct loss of material connected with crushing – both the dust loss, which resulted in less recovered materials, and untreated metal residues after combustion of the non-conductive fraction. Incineration and pyrolysis had very similar avoided impacts (−91.9 kg Cu eq. and −92.3 kg Cu eq, respectively). This similarity was expected because the final metal and silicon recovery were identical, the small difference likely came from the higher order hydrocarbons recovered in pyrolysis.

Another important aspect visible from Fig. 7 and the bars above the zero-line is the very similar impact of the separation methods. Except for US-swelling in UST-vol. all the panel-layer-separation units slightly

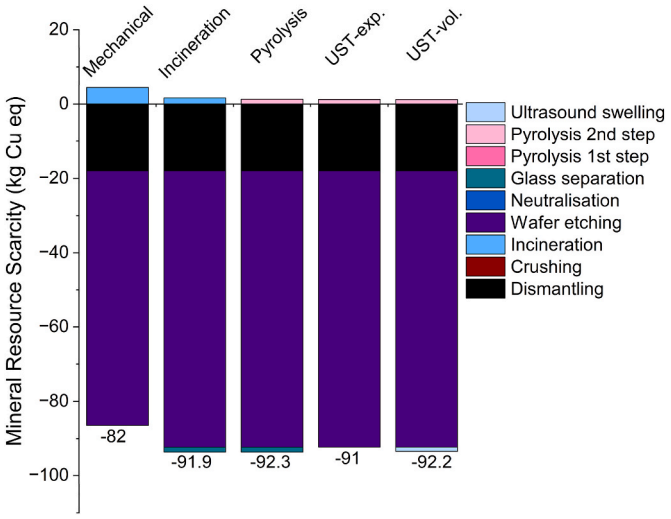

Fig. 7. Mineral resource scarcity per each unit operation of the five simulated variants based on the ReCiPe 2016H Midpoint methodologyö The numbers below the bars indicate the cumulative avoided environmental impact for each process (cumulative numbers do not correspond with the y-axis).

increase the global resource scarcity. The explanation for avoided impacts through US-swelling is that solar glass recovery through this unit outweighed other possible impacts. Furthermore, in all the processes the wafer etching and dismantling clearly had the highest contribution to the avoided mineral resources scarcity, because these stages recover single metallic species like copper, silver, tin oxide and lead oxide, or in the case of dismantling, the aluminium-alloy frame and the steel screws.

In summary, LCA analysis of the five recycling paths demonstrated that silicon solar panel recycling could avoid environmental impacts if the assumed material recovery and quality would have been reached. For instance, recovery of solar grade silicon was assumed, but if only metallurgical grade silicon was recovered, less impacts would be avoided. A similar statement could be made about the recovery of solar glass. Especially in the mechanical process, such an assumption is too optimistic since the glass is mixed with metals – the assumption was made nonetheless to enable facile analysis. However, it must be noted that the final quality of the recovered glass scrap is lower than the glass recovered from the UST and thermal processes.

4. Discussion

The main aim of this work was to compare different silicon solar panel recycling methods based on the analysis of exergy and environmental impacts. This helps navigate the development of recycling practices towards the United Nations Sustainable Development goal 12 – Responsible Consumption and Production [57] by providing the necessary background data. First, the mass-based recovery rates of the five simulated process variants – Incineration, Pyrolysis, UST-exp and -vol and Mechanical process were established. The material recovery of all the variants was found to be similar in this work based on the initial purity assumptions, only the Mechanical process had a slightly lower recovery rate due to material losses during crushing. However, the overall exergy efficiency (Fig. 5) of the simulated processes varied, indicating that exergy analysis is indispensable when comparing recycling approaches [30].

Interestingly, the form of recovered materials seems to matter - direct recovery of the frame (dismantling unit) or the whole glass (through hot-knife separation or UST-vol process) becomes exergy favourable, as evidenced by the exergy flows (Fig. 3) or irreversibility (Fig. 4). The mixing exergy was omitted in this analysis. However, accounting for it would have generally lowered the exergy content of mixed streams [31], thus penalizing especially the mechanical process. Since the irreversibility was comparable for all the glass liberation steps (shredding, US-swelling or hot-knife glass separation), it could be argued that recovering intact glass-sheets is advantageous. Otherwise, silicon, silver and copper had adequate purity for reintroduction into solar panel manufacturing [14].

However, the recovery of all or unbroken materials is not possible and exergy losses occurred. Such losses are unavoidable [28] if the objective is to recover solar grade silicon, pure metals, or intact glass. In theory more invested resources could increase the recovery at the given purity, but it would require thorough analysis to evaluate losses and benefits, as was done for other processes [30,48,49]. For now, irreversibility suggests a theoretical upper boundary for the exergy efficiency, assuming all recovered materials are useful.

Thus, the discrepancy between the exergy efficiency and the irreversibility was mainly based on the definition of useful products – in this study those were metals, the aluminium frame, clean glass, and solar grade silicon, based on their sufficient purity. The most profound example is the UST which has low irreversibility, but at the same time low exergy efficiency. The reason for this decoupling was the assumption that toluene is not a useful product. Similarly, during pyrolysis the overall efficiency of the process was lower than that of incineration while the total irreversibility was also lower. This is because irreversibility only describes the direct process losses through conversion of energy or chemical reactions, while it does not consider the usefulness of the process outputs. Therefore, the higher exergy of pyrolysis products than incineration off-gases results in lower irreversibility for pyrolysis, but the final efficiency of pyrolysis is lower due to its increased resource use compared to incineration.

Throughout the results, the encapsulant (EVA) of the solar panel could be linked with most of the exergy losses (see Figs. 3 and 4). Compared to metals, the exergy content of polymers is often higher [31], which resulted in higher irreversibility and higher exergy in waste streams. Similarly, the pyrolysis and incineration steps generally had the highest environmental impact, similarly to Latunussa et al. [36] where they also indicated incineration of EVA as one of the main contributors to GWP impacts in the recycling process. Such observations are important because significant resources are spent to get access to the silicon and metals. Which is discussed obstacle in silicon solar panel recycling [5,39]. After the liberation of these materials, all the following stages have direct useful products. One advantage of solar panels is that it is possible to access the cells without shredding [12,16,23]. This is important since the materials do not get mixed and the exergy is preserved, in contrast with shredding-based recycling [30,49,58].

Reiterating the previous observations, it could be argued that it is vital to use the exergy and LCA analyses in conjunction to understand the trade-offs in recycling approaches. For instance, in the mechanical process there was a direct link between lower recovery rate and lower exergy efficiency and avoided environmental impacts, relative to the other simulated processes. However, such link was not present for UST, pyrolysis, or incineration, which hinted that solely relying on the exergy analysis omits some of the environmental impacts. Exergy and LCA analysis together allowed to show that high resource consumption, as for example in UST, led to lower exergy efficiency and lower avoided impacts. On the other hand, using slightly more resources in pyrolysis compared to incineration could lead to an environmentally more advantageous recycling process. Yet gaseous emissions from pyrolysis, mainly CO – a toxic substance – and methane, a significant GWP contributor, would need to be treated to avoid significant harm. Furthermore, the expansion of the exergy analysis with LCA reinforces that high value recovery is advantageous, in agreement with findings of Mao et al. [39]. In summary, focusing only on exergy or LCA would fail to provide the detailed understanding of the differences between the processes covered in this work.

Contrasting with the work of Dias et al. [41] the path of lowering the toluene volume employed in this work was not as successful compared to scaled-up continuous operation. Contreras Lisperguer et al. [37] argued for solvent delamination to avoid environmental harm, yet present findings suggest caution when choosing the solvent. Building on [40], the LCA based comparison was expanded towards other techniques, putting mechanical recycling into broader perspective. The observations of Lim et al. [59] were further expanded herein by demonstrating that the adverse impact of recycling could be compensated by the replacement of primary materials, resulting in net avoided environmental impacts.

The robustness of the assumptions of energy inputs was tested as well, by considering the variation of exergy efficiency (see supplementary material section s11). For all the processes, the decrease or increase of the electricity input caused an exergy efficiency change of maximum 0.5 % compared to the initial efficiency. This shows that the assumptions about the energy inputs will not affect the outcome significantly. Thus, larger impact could be made through process optimization, as highlighted by the differences between UST-vol. and UST-exp., or by minimizing energy (heat) losses.

Lastly going beyond material recovery becomes important as recycling of solar panels slowly accelerates. Industrial scale recycling based on solvent swelling [41] seems to require subsidies to be profitable, yet it has technical potential to be scaled-up. Industrial scale pyrolysis-based recycling is operating in Europe on a start-up basis [60] and could become economically feasible [61,62] Mechanical recycling could be profitable for at least broken solar panels [20] on a large-scale basis. Thus, considering combined exergy-LCA assessments could be beneficial in providing additional insights for solar industry stakeholders and policy makers.

4.1. Pathways for improvement and study limitations

Based on the presented observations, a few pathways for decrease of energy losses could be sketched. For instance, the heat from the used toluene could be utilized to preheat the toluene entering the ultrasonic bath. In pyrolysis, the off-gases containing CH4 and CO could be utilized for chemical synthesis if further purified; the same applies to the liquor. Additionally, nitrogen coming into the pyrolysis oven could be preheated using the off-gases from pyrolysis. Where no recycling is possible, energy recovery would be an option, incinerating the pyrolysis off-gases and liquor for process heat, although this would increase direct CO_2 emissions. Lastly, the high-temperature heat in off-gas streams from incineration or pyrolysis could be used for preheating in the leaching and the glass-separation steps.

Another major improvement compared to the methods presented

herein would be the use limonene instead of toluene [63], because limonene could be derived from food residues [64]. By offering a lower chemical consumption of 10 ml/g sample (0.1M solution in ethanol) [63], this approach would provide a significant improvement in reducing the reagent's toxicity. Yet, due to the use of ultrasound, the impact of electricity consumption would remain. However, the treatment time could be lower for limonene-based swelling [63], offering a decrease in the total consumption. Thus, further work on the improvement of ultrasound-based techniques is required.

At this point it becomes essential to discuss limitations and possible improvements. The analysis presented here could benefit from the implementation of exergy of mixing and more detailed description of the state of the recovered materials, especially the impurities in recovered metals. This could also improve the LCA analysis, especially by including the remanufacturing of solar glass. Moreover, optimization of toluene use would be crucial to minimize chemical use and waste generation. All such improvements would likely result in more avoided impacts, pushing the positive impact of recycling even higher. However, future research could focus on the complex issue of purity of recovered materials and a sensitivity analysis with respect to that would expand the findings of the present work. With all its limitations the presented research demonstrates that exergy analysis and LCA enable a fair comparison of different silicon solar panel recycling approaches on a stage-by-stage basis.

5. Conclusion

This study set out to investigate how different methods of material separation from silicon solar panels compare based on theoretical exergy analysis and life cycle assessment. HSC chemistry™ was used to simulate four different separation methods to obtain process data. Using this data, an LCA analysis was conducted, which, in conjunction with exergy analysis, resulted in valuable insights.

The first main finding of this work is that despite the similar weight-based recovery of silicon, metals, and glass, the exergy efficiency and avoided impacts varied based on the separation method across the simulated processes. Generally, the direct thermal decomposition of the encapsulant (either through incineration or pyrolysis) performed the best out of the 5 process variants (UST-exp and -vol., Incineration, Pyrolysis and Mechanical processes). In contrast, the solvent based separation method exhibited the worst exergy efficiency and the least avoided impacts. In fact, it even resulted in adverse environmental impacts. However, utilizing natural solvents like limonene could lower these adverse impacts. In summary, the treatment of the encapsulant was generally the most resource intensive step based on this analysis.

The second major outcome is the demonstration of the importance of using exergy and LCA analysis in conjunction to assess the sustainability of the recycling approaches. For instance, pyrolysis only had the second highest exergy efficiency, but it resulted in the most avoided impacts out of the five process variants. This highlights that under certain conditions, a slightly less efficient process might be less harmful overall. On the other hand, there can be a clear link between material recovery rate, exergy efficiency and avoided environmental impacts, as was demonstrated for the mechanical recycling process. The main implication of these findings is that LCA and exergy analysis together can navigate towards more sustainable pathways to silicon solar panel recycling.

It is shown that these tools could also be used in the early stages of designing solar panel recycling process. Thus, it is recommended that solar panel manufacturers explore design-for-recycling based on the combined exergy-LCA methodology, facilitated by their access to industrial scale data. For example, lowering the mass of the encapsulant would result in lower exergy losses and a decrease in some of the adverse impacts. Secondly, this study highlights the importance of high-value material recovery for both policy makers and the industry. Therefore, this work, provides necessary scientific support for initiatives promoting sustainable design and r4ecycling practices, such as the EU eco-design directive.

Nevertheless, a potential avenue to be explored further is the inclusion of the exergy of mixing. This would add more granularity to the process understanding. Furthermore, studying the embodied exergy could bring value in understanding the benefits or losses in recovering intact materials. Similarly, the LCA could account for solar glass remanufacturing. Finally, this study could be the basis of solar panel designs that would increase the exergy efficiency of recycling and enhance the associated environmental benefits. Altogether the present research expanded the body of knowledge by highlighting the importance of combined exergy and LCA analysis in solar panel recycling. Such a combined analysis showed the potential benefits of recovering critical materials, avoiding unnecessary material destruction and recycling intact parts of the silicon solar panels.

CRediT authorship contribution statement

Šimon Jech: Writing – original draft, Visualization, Validation, Methodology, Investigation, Formal analysis, Conceptualization. **Neill Bartie:** Writing – review & editing, Validation, Methodology, Conceptualization. **Gulsah Tas:** Writing – original draft, Methodology, Investigation, Conceptualization. **Kati Miettunen:** Writing – review & editing, Funding acquisition, Conceptualization. **Rodrigo Serna-Guerrero:** Writing – review & editing, Formal analysis, Conceptualization. **Annukka Santasalo-Aarnio:** Writing – review & editing, Supervision, Methodology, Funding acquisition, Conceptualization.

Declaration of competing interest

The authors declare the following financial interests/personal relationships which may be considered as potential competing interests: Annukka Santasalo-Aarnio reports financial support was provided by Research Council of Finland. Kati Miettunen reports financial support was provided by Research Council of Finland. If there are other authors, they declare that they have no known competing financial interests or personal relationships that could have appeared to influence the work reported in this paper.

Acknowledgments

S.J., K.M. and A.S.-A. thank Research Council of Finland Project ECOSOL (numbers 347275 and 347276). S.J. wishes to thank the Aalto University School of Engineering for supporting this research. G.T. and R.S-G. thank the Finnish Natural Resources Research Foundation (Suomen Luonnonvarain Tutkimussäätiö) project CircuS for their support. The authors wish to acknowledge the help of Árpád I. Toldy in correcting the language and style of this article.

Appendix A. Supplementary data

Supplementary data to this article can be found online at https://doi.org/10.1016/j.solmat.2025.113561.

Data availability

Data will be made available on request.

References

[1] A.I. Osman, L. Chen, M. Yang, G. Msigwa, M. Farghali, S. Fawzy, D.W. Rooney, P. S. Yap, Cost, environmental impact, and resilience of renewable energy under a changing climate: a review, Environ. Chem. Lett. 21 (2023) 741–764, https://doi.org/10.1007/S10311-022-01532-8/METRICS.

[2] S. Weckend, A. Wade, G. Heath, END-OF-LIFE MANAGEMENT: SOLAR PHOTOVOLTAIC PANELS, 2016.

[3] European Commission, A new circular economy action plan for a cleaner and more competitive Europe, COM/2020/98 Final, https://eur-lex.europa.eu/legal-conte

nt/EN/TXT/?qid=1583933814386&uri=COM:2020:98:FIN, 2020. (Accessed 1 June 2022).
[4] M.A. Reuter, A. Van Schaik, J. Gutzmer, N. Bartie, A. Abadías-Llamas, Challenges of the circular economy: a material, metallurgical, and product design perspective, Annu. Rev. Mater. Res. 49 (2019) 253–274, https://doi.org/10.1146/ANNUREV-MATSCI-070218-010057/CITE/REFWORKS.
[5] C.C. Farrell, A.I. Osman, R. Doherty, M. Saad, X. Zhang, A. Murphy, J. Harrison, A. S.M. Vennard, V. Kumaravel, A.H. Al-Muhtaseb, D.W. Rooney, Technical challenges and opportunities in realising a circular economy for waste photovoltaic modules, Renew. Sustain. Energy Rev. 128 (2020), https://doi.org/10.1016/J.RSER.2020.109911.
[6] G.A. Heath, T.J. Silverman, M. Kempe, M. Deceglie, D. Ravikumar, T. Remo, H. Cui, P. Sinha, C. Libby, S. Shaw, K. Komoto, K. Wambach, E. Butler, T. Barnes, A. Wade, Research and development priorities for silicon photovoltaic module recycling to support a circular economy, Nat. Energy 5 (2020) 502–510, https://doi.org/10.1038/s41560-020-0645-2.
[7] J.A. Tsanakas, A. van der Heide, T. Radavičius, J. Denafas, E. Lemaire, K. Wang, J. Poortmans, E. Voroshazi, Towards a circular supply chain for PV modules: review of today's challenges in PV recycling, refurbishment and re-certification, Prog. Photovoltaics Res. Appl. 28 (2020) 454–464, https://doi.org/10.1002/PIP.3193.
[8] G. Thomassen, J. Dewulf, S. Van Passel, Prospective material and substance flow analysis of the end-of-life phase of crystalline silicon-based PV modules, Resour. Conserv. Recycl. 176 (2022), https://doi.org/10.1016/J.RESCONREC.2021.105917.
[9] Directive 2012/19/EU, directive 2012/19/EU of the European parliament and of the Council of 4 july 2012 on waste electrical and electronic equipment (WEEE). https://eur-lex.europa.eu/legal-content/EN/TXT/?uri=CELEX%3A02012L0019-20240408, 2024. (Accessed 19 June 2024).
[10] A. Lennon, M. Lunardi, B. Hallam, P.R. Dias, The aluminium demand risk of terawatt photovoltaics for net zero emissions by 2050, Nat. Sustain. 5 (2022) 357–363, https://doi.org/10.1038/s41893-021-00838-9.
[11] S. Preet, S.T. Smith, A comprehensive review on the recycling technology of silicon based photovoltaic solar panels: challenges and future outlook, J. Clean. Prod. 448 (2024) 141661, https://doi.org/10.1016/J.JCLEPRO.2024.141661.
[12] R. Wang, E. Song, C. Zhang, X. Zhuang, E. Ma, J. Bai, W. Yuan, J. Wang, Pyrolysis-based separation mechanism for waste crystalline silicon photovoltaic modules by a two-stage heating treatment, RSC Adv. 9 (2019) 18115–18123, https://doi.org/10.1039/C9RA03582F.
[13] Z. De-Wen, M. Born, K. Wambach, Pyrolysis of EVA and its application in recycling of photovoltaic modules, J. Environ. Sci. 16 (2004) 889–893.
[14] W.H. Huang, W.J. Shin, L. Wang, W.C. Sun, M. Tao, Strategy and technology to recycle wafer-silicon solar modules, Sol. Energy 144 (2017) 22–31, https://doi.org/10.1016/J.SOLENER.2017.01.001.
[15] T.Y. Wang, J.C. Hsiao, C.H. Du, Recycling of materials from silicon base solar cell module. 2012 38th IEEE Photovoltaic Specialists Conference, 2012, pp. 2355–2358, https://doi.org/10.1109/PVSC.2012.6318071.
[16] Y. Kim, J. Lee, Dissolution of ethylene vinyl acetate in crystalline silicon PV modules using ultrasonic irradiation and organic solvent, Sol. Energy Mater. Sol. Cell. 98 (2012) 317–322, https://doi.org/10.1016/j.solmat.2011.11.022.
[17] M.F. Azeumo, C. Germana, N.M. Ippolito, M. Franco, P. Luigi, S. Settimio, Photovoltaic module recycling, a physical and a chemical recovery process, Sol. Energy Mater. Sol. Cell. 193 (2019) 314–319, https://doi.org/10.1016/j.solmat.2019.01.035.
[18] T. Doi, I. Tsuda, H. Unagida, A. Murata, K. Sakuta, K. Kurokawa, Experimental study on PV module recycling with organic solvent method, Sol. Energy Mater. Sol. Cell. 67 (2001) 397–403, https://doi.org/10.1016/S0927-0248(00)00308-1.
[19] H. Kumar Trivedi, A. Meshram, R. Gupta, Removal of encapsulant Ethylene-vinyl acetate (EVA) from solar cells of photovoltaic modules (PVMs), Mater. Today Proc. (2023), https://doi.org/10.1016/J.MATPR.2023.08.109.
[20] P.R. Dias, L. Schmidt, N.L. Chang, M. Monteiro Lunardi, R. Deng, B. Trigger, L. Bonan Gomes, R. Egan, H. Veit, High yield, low cost, environmentally friendly process to recycle silicon solar panels: technical, economic and environmental feasibility assessment, Renew. Sustain. Energy Rev. 169 (2022) 112900, https://doi.org/10.1016/j.rser.2022.112900.
[21] J. Li, S. Yan, Y. Li, Z. Wang, Y. Tan, J. Li, M. Xia, P. Li, Recycling Si in waste crystalline silicon photovoltaic panels after mechanical crushing by electrostatic separation, J. Clean. Prod. 415 (2023) 137908, https://doi.org/10.1016/J.JCLEPRO.2023.137908.
[22] S.M. Nevala, J. Hamuyuni, T. Junnila, T. Sirviö, S. Eisert, B.P. Wilson, R. Serna-Guerrero, M. Lundström, Electro-hydraulic fragmentation vs conventional crushing of photovoltaic panels – impact on recycling, Waste Manag. 87 (2019) 43–50, https://doi.org/10.1016/j.wasman.2019.01.039.
[23] R. Frischknecht, K. Komoto, T. Doi, Life cycle assessment of crystalline silicon photovoltaic module delamination with hot knife technology. https://iea-pvps.org/key-topics/life-cycle-assessment-of-crystalline-silicon-photovoltaic-module-delamination-with-hot-knife-technology/, 2023. (Accessed 28 June 2024).
[24] S. Jech, N. Garg, A. Santasalo-Aarnio, K. Miettunen, Comparison of experimental separation methods for silicon solar panels, EU PVSEC Proceedings (2023), https://doi.org/10.4229/EUPVSEC2023/5DV.2.37.
[25] M.A. Reuter, A. Van Schaik, J. Gutzmer, N. Bartie, A. Abadías-Llamas, Challenges of the circular economy: a material, metallurgical, and product design perspective, Annu. Rev. Mater. Res. 49 (2019) 253–274, https://doi.org/10.1146/ANNUREV-MATSCI-070218-010057.
[26] L. Gai, S. Varbanov, Y. Van Fan, J.J. Klemeš, V. Romanenko, Trade-offs between the recovery, exergy demand and economy in the recycling of multiple resources, Resour. Conserv. Recycl. (2021), https://doi.org/10.1016/j.resconrec.2021.105428.
[27] C. Ballif, F.J. Haug, M. Boccard, P.J. Verlinden, G. Hahn, Status and perspectives of crystalline silicon photovoltaics in research and industry, Nat. Rev. Mater. 7 (8 7) (2022) 597–616, https://doi.org/10.1038/s41578-022-00423-2, 2022.
[28] M.A. Reuter, A. Van Schaik, O. Ignatenko, G.J. De Haan, Fundamental limits for the recycling of end-of-life vehicles, Miner. Eng. 19 (2006) 433–449, https://doi.org/10.1016/J.MINENG.2005.08.014.
[29] P. Wollants, Thermodynamics 101, handbook of recycling, 545–554, https://doi.org/10.1016/B978-0-12-396459-5.15002-0, 2014.
[30] O. Ignatenko, A. van Schaik, M.A. Reuter, Exergy as a tool for evaluation of the resource efficiency of recycling systems, Miner. Eng. 20 (2007) 862–874, https://doi.org/10.1016/j.mineng.2007.03.005.
[31] J. Szargut, D.R. Morris, F.R. Steward, Exergy Analysis of Thermal, Chemical, and Metallurgical Processes, 1987.
[32] N.J. Bartie, Y.L. Cobos-Becerra, M. Fröhling, R. Schlatmann, M.A. Reuter, The resources, exergetic and environmental footprint of the silicon photovoltaic circular economy: assessment and opportunities, Resour. Conserv. Recycl. 169 (2021) 105516, https://doi.org/10.1016/J.RESCONREC.2021.105516.
[33] N.J. Bartie, A. Abadías Llamas, M. Heibeck, M. Fröhling, O. Volkova, M.A. Reuter, The simulation-based analysis of the resource efficiency of the circular economy – the enabling role of metallurgical infrastructure, Miner. Process. Extr. Metall. (IMM Trans. Sect. C) 129 (2020) 229–249, https://doi.org/10.1080/25726641.2019.1685243.
[34] N. Bartie, L. Cobos-Becerra, F. Mathies, J. Dagar, E. Unger, M. Fröhling, M. A. Reuter, R. Schlatmann, Cost versus environment? Combined life cycle, techno-economic, and circularity assessment of silicon- and perovskite-based photovoltaic systems, J. Ind. Ecol. 27 (2023) 993–1007, https://doi.org/10.1111/JIEC.13389.
[35] J. Gediga, Life-cycle assessment, handbook of recycling, 555–562, https://doi.org/10.1016/B978-0-12-396459-5.15003-2, 2014.
[36] C.E.L. Latunussa, F. Ardente, G.A. Blengini, L. Mancini, Life Cycle Assessment of an innovative recycling process for crystalline silicon photovoltaic panels, Sol. Energy Mater. Sol. Cell. 156 (2016) 101–111, https://doi.org/10.1016/J.SOLMAT.2016.03.020.
[37] R. Contreras Lisperguer, E. Muñoz Cerón, J. de la Casa Higueras, R.D. Martín, Environmental impact assessment of crystalline solar photovoltaic panels' end-of-life phase: open and closed-loop material flow scenarios, Sustain. Prod. Consum. 23 (2020) 157–173, https://doi.org/10.1016/J.SPC.2020.05.008.
[38] M.S.W. Lim, D. He, J.S.M. Tiong, S. Hanson, T.C.K. Yang, T.J. Tiong, G.T. Pan, S. Chong, Experimental, economic and life cycle assessments of recycling end-of-life monocrystalline silicon photovoltaic modules, J. Clean. Prod. 340 (2022) 130796, https://doi.org/10.1016/J.JCLEPRO.2022.130796.
[39] D. Mao, S. Yang, L. Ma, W. Ma, Z. Yu, F. Xi, J. Yu, Overview of life cycle assessment of recycling end-of-life photovoltaic panels: a case study of crystalline silicon photovoltaic panels, J. Clean. Prod. 434 (2024) 140320, https://doi.org/10.1016/j.jclepro.2023.140320.
[40] A. Heiho, I. Suwa, Y. Dou, S. Lim, T. Namihira, T. Koita, K. Mochidzuki, S. Murakami, I. Daigo, C. Tokoro, Y. Kikuchi, Prospective life cycle assessment of recycling systems for spent photovoltaic panels by combined application of physical separation technologies, Resour. Conserv. Recycl. 192 (2023) 106922, https://doi.org/10.1016/J.RESCONREC.2023.106922.
[41] P. Dias, L. Schmidt, M. Monteiro Lunardi, N.L. Chang, G. Spier, R. Corkish, H. Veit, Comprehensive recycling of silicon photovoltaic modules incorporating organic solvent delamination – technical, environmental and economic analyses, Resour. Conserv. Recycl. 165 (2021) 105241, https://doi.org/10.1016/J.RESCONREC.2020.105241.
[42] Metso, HSC Chemistry™, 2024.
[43] Greendelta GmbH, OpenLCA, 2024.
[44] ecoinvent, Ecoinvent Database, 2024.
[45] J. Shin, J. Park, N. Park, A method to recycle silicon wafer from end-of-life photovoltaic module and solar panels by using recycled silicon wafers, Sol. Energy Mater. Sol. Cell. 162 (2017) 1–6, https://doi.org/10.1016/j.solmat.2016.12.038.
[46] J. Park, W. Kim, N. Cho, H. Lee, N. Park, An eco-friendly method for reclaimed silicon wafers from a photovoltaic module: from separation to cell fabrication, Green Chem. 18 (2016) 1706–1714, https://doi.org/10.1039/C5GC01819F.
[47] Metso, Exergy balance module - HSC chemistry. https://www.metso.com/globalassets/portfolio/hsc-chemistry/15-exergy-balance.pdf, 2024. (Accessed 10 September 2024).
[48] M. Vierunketo, A. Klemettinen, M.A. Reuter, A. Santasalo-Aarnio, R. Serna-Guerrero, A grave-to-cradle analysis of lithium-ion battery cathode materials using material and energy circularity indicators, J. Clean. Prod. 471 (2024) 143435, https://doi.org/10.1016/J.JCLEPRO.2024.143435.
[49] M. Vierunketo, A. Klemettinen, M.A. Reuter, A. Santasalo-Aarnio, R. Serna-Guerrero, A multi-dimensional indicator for material and energy circularity: proof-of-concept of exentropy in Li-ion battery recycling, iScience 26 (2023) 108237, https://doi.org/10.1016/J.ISCI.2023.108237.
[50] D.W. Van Krevelen, K. Te Nijenhuis, Properties of Polymers, fourth ed., Elsevier, Amsterdam, 2009.
[51] T.J. Kotas, The Exergy Method of Thermal Plant Analysis, Elsevier, 1985, https://doi.org/10.1016/C2013-0-00894-8.
[52] Y. Tang, J. Dong, Y. Chi, Z. Zhou, M. Ni, Energy and exergy analyses of fluidized-bed municipal solid waste air gasification, Energy & Fuels 30 (2016) 7629–7637, https://doi.org/10.1021/acs.energyfuels.6b01418.
[53] V.A. Benignus, Health effects of toluene: a review, Neurotoxicology 2 (1981) 567–588. https://europepmc.org/article/med/7038560/reload=0 (accessed June 4, 2023).

[54] C. Farrell, A.I. Osman, X. Zhang, A. Murphy, R. Doherty, K. Morgan, D.W. Rooney, J. Harrison, R. Coulter, D. Shen, Assessment of the energy recovery potential of waste photovoltaic (pV) modules, Nature Scientific Reports 9 (2019), https://doi.org/10.1038/s41598-019-41762-5.
[55] S.H. Amini, J.A.M. Remmerswaal, M.B. Castro, M.A. Reuter, Quantifying the quality loss and resource efficiency of recycling by means of exergy analysis, J. Clean. Prod. 15 (2007) 907–913, https://doi.org/10.1016/J.JCLEPRO.2006.01.010.
[56] M.B.G. Castro, J.A.M. Remmerswaal, J.C. Brezet, M.A. Reuter, Exergy losses during recycling and the resource efficiency of product systems, Resour. Conserv. Recycl. 52 (2007) 219–233, https://doi.org/10.1016/j.resconrec.2007.01.014.
[57] United Nations, Goal 12, Department of Economic and Social Affairs, 2024. https://sdgs.un.org/goals/goal12. (Accessed 16 January 2025).
[58] O. Velázquez-Martínez, J. Valio, A. Santasalo-Aarnio, M. Reuter, R. Serna-Guerrero, A critical review of lithium-ion battery recycling processes from a circular economy perspective, Batteries 5 (2019) 5–7, https://doi.org/10.3390/batteries5040068.
[59] M.S.W. Lim, D. He, J.S.M. Tiong, S. Hanson, T.C.K. Yang, T.J. Tiong, G.T. Pan, S. Chong, Experimental, economic and life cycle assessments of recycling end-of-life monocrystalline silicon photovoltaic modules, J. Clean. Prod. 340 (2022) 130796, https://doi.org/10.1016/J.JCLEPRO.2022.130796.
[60] C. Salas-Redondo, S. Bade, A. Chalaux, Y. Luo, Recycled silicon for chlorosilane production, SSRN Electron. J. (2024), https://doi.org/10.2139/SSRN.4943277.
[61] G. Granata, P. Altimari, F. Pagnanelli, J. De Greef, Recycling of solar photovoltaic panels: techno-economic assessment in waste management perspective, J. Clean. Prod. 363 (2022) 132384, https://doi.org/10.1016/J.JCLEPRO.2022.132384.
[62] R. Deng, N.L. Chang, Z. Ouyang, C.M. Chong, A techno-economic review of silicon photovoltaic module recycling, Renew. Sustain. Energy Rev. 109 (2019) 532–550, https://doi.org/10.1016/J.RSER.2019.04.020.
[63] R. Min, W. Deng, Z. Wang, T. Qi, Z. Zhang, W. Xiao, G. Qian, D. Wang, Effective decapsulation method for photovoltaic modules: limonene-induced EVA controlled swelling under sonication and debonding mechanism analysis, J. Clean. Prod. 450 (2024) 141917, https://doi.org/10.1016/J.JCLEPRO.2024.141917.
[64] G. Paggiola, S. Van Stempvoort, J. Bustamante, J.M.V. Barbero, A.J. Hunt, J. H. Clark, Can bio-based chemicals meet demand? Global and regional case-study around citrus waste-derived limonene as a solvent for cleaning applications, Biofuels, Bioproducts and Biorefining 10 (2016) 686–698, https://doi.org/10.1002/BBB.1677.